Expression of Mutant Myocilin Induces Abnormal Intracellular Accumulation of Selected Extracellular Matrix Proteins in the Trabecular Meshwork

Ramesh B. Kasetti, Tien N. Phan, J. Cameron Millar, and Gulab S. Zode

North Texas Eye Research Institute, University of North Texas Health Science Center at Fort Worth, Texas, United States

Correspondence: Gulab S. Zode, North Texas Eye Research Institute, CBH-413, University of North Texas Health Science Center, 3500 Camp Bowie Boulevard, Ft. Worth, TX 76107, USA; gulab.zode@unthsc.edu.

Submitted: March 21, 2016
Accepted: October 3, 2016

Citation: Kasetti RB, Phan TN, Millar JC, Zode GS. Expression of mutant myocilin induces abnormal intracellular accumulation of selected extracellular matrix proteins in the trabecular meshwork. *Invest Ophthalmol Vis Sci*. 2016;57:6058–6069. DOI:10.1167/iovs.16-19610

Purpose. Abnormal accumulation of extracellular matrix (ECM) in the trabecular meshwork (TM) is associated with decreased aqueous humor outflow facility and IOP elevation in POAG. Previously, we have developed a transgenic mouse model of POAG (*Tg-MYOC^{Y437H}*) by expressing human mutant myocilin (MYOC), a known genetic cause of POAG. The purpose of this study is to examine whether expression of mutant myocilin leads to reduced outflow facility and abnormal ECM accumulation in *Tg-MYOC^{Y437H}* mice and in cultured human TM cells.

Methods. Conscious IOP was measured at various ages of *Tg-MYOC^{Y437H}* mice using a rebound tonometer. Outflow facility was measured in 10-month-old *Tg-MYOC^{Y437H}* mice. Selected ECM proteins were examined in human TM-3 cells stably expressing mutant myocilin and primary human TM cells ($n = 4$) as well as in the TM of *Tg-MYOC^{Y437H}* mice by real-time PCR, Western blotting, and immunostaining. Furthermore, TM cells expressing WT or mutant myocilin were treated with 5 mM sodium 4-phenylbutyrate (PBA), and ECM proteins were examined by Western blot and immunostaining.

Results. Starting from 3 months of age, *Tg-MYOC^{Y437H}* mice exhibited significant IOP elevation compared with wild-type (WT) littermates. Outflow facility was significantly reduced in *Tg-MYOC^{Y437H}* mice (0.0195 µl/min/mm Hg in *Tg-MYOC^{Y437H}* vs. 0.0332 µl/min/mm Hg in WT littermates). Increased accumulation of fibronectin, elastin, and collagen type IV and I was observed in the TM of *Tg-MYOC^{Y437H}* mice compared with WT littermates. Furthermore, increased ECM proteins were also associated with induction of endoplasmic reticulum (ER) stress markers, GRP78 and CHOP in the TM of *Tg-MYOC^{Y437H}* mice. Human TM-3 cells stably expressing DsRed-tagged Y437H mutant MYOC exhibited inhibition of myocilin secretion and its intracellular accumulation compared with TM cells expressing WT MYOC. Expression of mutant MYOC in TM-3 cells or human primary TM cells induced ER stress and also increased intracellular protein levels of fibronectin, elastin, laminin, and collagen IV and I. In addition, TM-3 cells expressing mutant myocilin exhibited reduced active forms of matrix metalloproteinase (MMP)-2 and MMP-9 in conditioned medium compared with TM-3 cells expressing WT myocilin. Interestingly, both intracellularly accumulated fibronectin and collagen I colocalized with mutant myocilin and also with ER marker KDEL further suggesting intracellular accumulation of these proteins in the ER of TM cells. Furthermore, reduction of ER stress via PBA decreased selected ECM proteins in primary TM cells.

Conclusions. These studies demonstrate that mutant myocilin induces abnormal ECM accumulation in the ER of TM cells, which may be responsible for reduced outflow facility and IOP elevation in myocilin-associated glaucoma.

Keywords: myocilin, ECM, glaucoma, trabecular meshwork, ER stress

Glaucoma is a leading cause of irreversible blindness affecting approximately 70 million people worldwide. Primary open angle glaucoma (POAG) is the most common form of glaucoma and is characterized by progressive loss of retinal ganglion cell (RGC) axons and irreversible loss of vision.[1,2] Elevated IOP is a major associated risk factor, and the only treatable risk factor.[3] The trabecular meshwork (TM) maintains normal IOP by regulating outflow resistance. In POAG, there is increased resistance to aqueous humor outflow through the trabecular meshwork (TM), thus elevating IOP.[4,5] The glaucomatous TM damage is associated with various morphologic and biochemical changes including abnormal extracellular matrix (ECM) protein accumulation[5–8] and loss of TM cells.[9] Increased expression of ECM proteins including fibronectin, collagen type IV, elastin, and laminin have been reported in the glaucomatous TM tissues.[8,10,11] Extracellular matrix composition is further tightly regulated by matrix metalloproteinase (MMP) activity. Although several MMPs are expressed in the TM, MMP-2 and MMP-9 are well studied in TM cells.[12–16] In addition, reorganization of actin microfilaments to form cross-linked actin networks is also associated with glaucomatous TM cells and tissues.[17,18] Increased accumulation

Investigative Ophthalmology & Visual Science

of ECM proteins in the TM is thought to be responsible for increased aqueous humor outflow resistance (or reduced outflow facility), thus elevating IOP.[5,11,14]

Myocilin (MYOC) mutations resulting in elevated IOP are responsible for approximately 4% of POAG and most cases of autosomal dominant juvenile-onset-open-angle glaucoma.[4,19] Although the exact role of wild type (WT) MYOC is not completely understood, myocilin appears to be released into the ECM as exosomes and may have an extracellular function.[20–22] Wild-type myocilin has been shown to interact with fibronectin in vitro.[23] In addition, myocilin appears to colocalize with fibronectin, collagen type IV, and laminin in cultured TM cells treated with dexamethasone (Dex). Several in vitro studies demonstrated that disease-causing MYOC mutants are secretion incompetent and accumulate in the endoplasmic reticulum (ER), inducing ER stress.[24–32] Using *Tg-MYOC^{Y437H}* mice expressing mutant human myocilin, we have shown that ER stress is associated with IOP elevation in MYOC-associated glaucoma.[26] We have recently demonstrated that ER stress is also associated with glucocorticoid-induced ocular hypertension.[33]

Extracellular matrix proteins are synthesized in the ER, modified and matured in the golgi, and secreted and assembled into the ECM. Malfunction of ER homeostasis during chronic ER stress may alter ECM protein processing and secretion. Because mutant myocilin accumulates in the ER as aggregates and disrupts normal ER homeostasis, it is conceivable that protein misfolding and ER stress may alter folding and processing of several other secreted proteins including ECM proteins. We therefore hypothesize that mutant myocilin leads to abnormal intracellular accumulation of ECM proteins in the TM, which may further aggravate ER stress, causing TM dysfunction and reduced outflow facility, thereby elevating IOP. In the present study, we sought to examine the effect of mutant myocilin expression on outflow facility and ECM remodeling in cultured human TM cells and in *Tg-MYOC^{Y437H}* mice. Previously, WT myocilin has been shown to interact with fibronectin, and myocilin colocalized with fibronectin, collagen type IV, and laminin in TM cells treated with Dex.[23] Therefore, we particularly examined the effects of mutant myocilin on synthesis and secretion of these selected ECM proteins in human TM cells and in *Tg-MYOC^{Y437H}* mice.

Materials and Methods

Mouse Husbandry

A detailed characterization of *Tg-MYOC^{Y437H}* mice has been published previously.[26] *Tg-MYOC^{Y437H}* mice on C57BL/6J background were crossed with pure strain AJ mice and F2 mice were intercrossed. The mice were genotyped by PCR with primers specific to human MYOC, as described previously.[26] Age-matched WT and *Tg-MYOC^{Y437H}* littermates were used for phenotype study and further biochemical analysis. Animals were fed standard chow ad libitum and kept in 12-hour light/12-hour dark conditions. All experimental procedures were conducted in accordance with and adherence to the ARVO Statement for the Use of Animals in Ophthalmic and Vision Research, and the University of North Texas Health Science Center (UNTHSC; Fort Worth, TX, USA) Institutional Animal Care and Use Committee (IACUC) Regulations and Guidelines.

Antibodies

Antibodies were purchased from the following sources: fibronectin (catalog # Ab2413; Abcam, Cambridge, MA, USA), KDEL (catalog # Ab12223; Abcam), Collagen type I (catalog # NB600-408; Novus Biologicals, Littleton, CO, USA), Collagen type IV (catalog # SAB4500369; Sigma-Aldrich Corp., St. Louis, MO, USA), Laminin (catalog # L9393; Sigma-Aldrich), Elastin (catalog # MAB 2503; Millipore, Billerica, MA, USA), Myocilin (catalog # SC-21243; Santa Cruz Biotechnology, Dallas, TX, USA), ATF-4 (C/EBP-homologous protein; catalog # Sc-200, Santa Cruz Biotechnology), CHOP (catalog # 13172, Novus Biologicals), MMP-2 (catalog # NB200-193; Novus Biologicals), MMP-9 (catalog # SC-10737; Santa Cruz Biotechnology), and GAPDH (Glyceraldehyde 3-phosphate dehydrogenase; catalog # 3683; Cell Signaling Technology, Danvers, MA, USA).

IOP Measurement

Intraocular pressure was determined in behaviorally trained mice using a TonoLab rebound tonometer (Colonial Medical Supply, Windham, NH, USA), as described previously.[34] Daytime IOP was measured between 1 PM and 4 PM. A total of six individual IOP measurements were recorded. The mean ± SEM of the recorded readings was then calculated as the final IOP value for each eye. All IOP measurements were recorded in a masked manner. Intraocular pressure was measured in six mice ($n = 12$) at 3 and 8 months of age and each eye was considered as an individual value ($n = 2$ per mice).

Aqueous Humor Outflow Facility

Aqueous humor outflow facility was measured in each animal by constant flow infusion, following our previously published methodology.[35,36] Briefly, a total of four age-matched WT and *Tg-MYOC^{Y437H}* littermates ($n = 8$ eyes) were anesthetized (ketamine 100mg/kg; xylazine 10 mg/kg, intraperitoneal injection). After development of a suitable plane of surgical anesthesia, the anterior chamber was cannulated with a 30-G steel needle connected to a flow-through pressure transducer (BLPR; World Precision Instruments [WPI], Sarasota, FL, USA) for the continuous determination of pressure within the system. The opposing end of the pressure transducer was connected to a 1-mL syringe filled with sterile PBS (filtered through a 0.2-μm PALL HT Tuffryn Membrane Acrodisc Syringe Filter; Gelman Laboratory, Port Washington, NY, USA) loaded into a microdialysis infusion pump (SP101i; WPI). Signals from the pressure transducer were passed via a bridge amplifier (TBM4M; WPI) using the maximum gain setting (×1000), and an analog-to-digital converter (Lab-Trax; WPI) to a computer. Data were recorded using suitable software (LabScribe2; WPI). Following equilibration (taking typically 20–30 minutes following anterior chamber cannulation), eyes were infused at a flow rate of 0.1 μL/min. When pressure had stabilized (typically within 10–15 minutes), flow rate was increased sequentially to 0.2, 0.3, 0.4, and 0.5 μL/min. Three stabilized pressures at each flow rate were recorded, and the mean value calculated as the final stabilized pressure. Outflow facility was calculated as the reciprocal of the slope of a plot of measured pressure as ordinate against flow rate as abscissa. Following outflow facility measurements, animals were euthanized without being allowed to recover consciousness.

TM Cell Cultures

Human primary TM cells obtained from four different donors and transformed GTM-3 cells were cultured and characterized as described previously.[37] Briefly, TM cells were cultured in Dulbecco's modified Eagle's medium (DMEM) with L-glutamine (0.292 mg/mL; Invitrogen-Gibco, Grand Island, NY, USA), penicillin (100 units/mL)/streptomycin (0.1 mg/mL; Invitrogen-Gibco), and 10% fetal bovine serum (FBS; Invitrogen,

Investigative Ophthalmology & Visual Science

Grand Island, NY, USA). TM-3 cells stably expressing DsRed-tagged WT or mutant myocilin were generated by transient transfection with pDsRED2-MYOC plasmids and selection of colonies using G418 antibiotics (0.6 mg/ml; Gibco, Life Technologies, Grand Island, NY, USA). Stable cells expressing WT or mutant MYOC were maintained in DMEM containing G418 antibiotics. To examine the effect of mutant myocilin on ECM proteins, TM-3 cells stably expressing WT or mutant myocilin were grown in DMEM with 0%, 2%, and 10% FBS. Cellular lysates and conditioned medium were subjected for Western blot analysis of ECM proteins. In addition, TM-3 cells stably expressing WT or mutant myocilin cultured in serum-free medium were fixed after 24 hours and immunostained for fibronectin (FN) and collagen type I (Col I). Colocalization of fibronectin and myocilin were examined using a confocal microscope. For collection of conditioned medium, TM cells were cultured in 12-well plates with 0%, 2%, or 10% FBS (2-mL media) for 48 hours. Total medium was collected and centrifuged at 20817*g* for 15 minutes to remove dead cells and debris. Equal volumes of supernatant (1 mL) for each treatment were mixed with 10-µl resin (StrataClean Resin; Agilent, Inc., Santa Clara, CA, USA) to concentrate medium as described previously.[38,39] Samples were rotated overnight at 4°C. Next day, samples were centrifuged at 20817*g* for 5 minutes and lithium dodecyl sulphate sample buffer was added to pellet and subjected to SDS-PAGE. Coomassie staining was performed to ensure equal protein loading as described previously.[33] It should be noted that only the soluble forms (not cross-linked) of secreted ECM are detected by Western blot analysis.

To study the effect of mutant myocilin in human primary TM cells, TM cells obtained from four different donors were transfected using nucleofector electroporation with conditions optimized for TM cells as described previously.[40] Briefly, approximately 1×10^6 cells were nucleofected with pDsRED2-MYOC plasmids using the Amaxa 4D Nucleofector (program CA167) and P5 Primary cell 4D Nucleofector kit according to the manufacturer's instructions (Lonza, Allendale, NJ, USA). The cells were transferred back to culture dishes and cultured for 7 days post nucleofection. Approximately 40% to 50% of cells expressed DsRed WT or mutant myocilin with minimal cell death (less than 5%). Cells were maintained in serum-free medium for 48 hours and conditioned medium was subjected to Western blot analysis for ECM proteins and cells were fixed with 4% paraformaldehyde for 15 minutes. Colocalization of fibronectin and myocilin were examined using confocal microscope (Leica, Buffalo Grove, IL, USA). To study colocalization of fibronectin and collagen I with KDEL, confluent primary human TM cells were transduced with adenovirus (Ad) 5 expressing WT or Y437H mutant myocilin for 48 hours ($n = 4$ cell strains) in serum-free medium. For treatment with sodium 4-phenylbutyrate (PBA), TM cells were transduced with Ad5 WT or mutant myocilin and incubated with or without PBA (5 mM) for 48 hours in presence of 10% serum. Cell lysates and fixed TM cells were used for analysis of ECM synthesis and secretion in the TM. Pharmaceutical-grade 4-PBA was purchased from Scandinavian Formulas (Scandinavian Formulas, Inc., Sellersville, PA, USA).

Immunostaining

Mouse eyes from age-matched WT and *Tg-MYOC^{Y437H}* littermates were enucleated, fixed in 4% paraformaldehyde for 3 hours, and cryoprotected by keeping fixed eyes in 30% sucrose overnight before optimum cutting temperature embedding. Sections of 10-µm thickness were made using a cryostat (Leica Biosystems, Inc., Buffalo Grove, IL, USA). The sections were allowed to dry at room temperature prior to use. The sections were then permeabilized using 0.1% Triton X-100 in 1X PBS for 15 minutes and blocked with 10% normal goat serum for 1 hour. Slides were incubated overnight with primary antibody (1:100) and washed three times with PBS followed by 2-hour incubation in appropriate Alexa Fluor secondary antibodies (1:200; Invitrogen). Sections were mounted with 4′,6-diamidino-2-phenylindole (DAPI)-mounting solution. Images were captured using a Leica confocal imaging system. For immunostaining of TM cells, TM cells were fixed in 4% paraformaldehyde for 10 minutes, permeabilized with 0.1% Triton X-100 for 10 minutes and stained with antibodies specific to ECM proteins as described above.

Western Blot Analysis

Mouse anterior segments were carefully dissected from enucleated eyes and homogenized in 1X lysis buffer (200 µL) containing HEPES (50 mM), KCl (200 mM), EDTA (2 mM), $MgCl_2$ (1 mM), Triton X-100 (0.5%), glycerol (10%), 0.5 mM dithiothreitol and protease inhibitor cocktail tablets (Roche Life Sciences, Indianapolis, IN, USA) as described previously.[33] Total lysate was centrifuged at 20817*g* for 15 minutes and supernatant was subjected to protein concentration measurement using the DC Protein Assay from Bio-Rad (Hercules, CA, USA). Approximately 120 µg of total protein can be obtained from each eye. Thirty micrograms of total protein lysates were subjected to SDS-PAGE on denaturing 4-12% gradient polyacrylamide ready-made gels (NuPAGE Bis-Tris gels; Life Technologies) and transferred onto polyvinylylidene difluoride membranes. Blots were blocked with 10% non-fat dried milk for 1 hour then incubated overnight with specific primary antibodies at 4°C on a rotating shaker. The membranes were washed thrice with phosphate buffered saline with tween 20 (PBST) and incubated with the corresponding HRP-conjugated secondary antibody. The proteins were then visualized in Odessy Fc Imaging system (LI-COR, Lincoln, NE, USA) using ECL detection reagents (SuperSignal West Femto Maximum Sensitivity Substrate; Pierce Biotechnology, Grand Island, NY, USA). Densitometric analysis of Western blot was carried out using ImageJ software (http://imagej.nih.gov/ij/; provided in the public domain by the National Institutes of Health, Bethesda, MD, USA)

Quantitative Real-Time PCR

Real-time PCR was performed as described previously.[8] The mouse eyes were enucleated from age-matched WT and *Tg-MYOC^{Y437H}* littermates ($n = 5$). The TM rings were carefully dissected in such a way that the TM rings contained mainly TM tissue and only small amounts of sclera or cornea. Tissues were homogenized and total RNA was extracted using TRIzol reagent (Invitrogen). First strand cDNA synthesis was carried out using a Bio-Rad iScript cDNA synthesis Kit (Bio-Rad). Each PCR reaction contained: 10 µL 2X iQ SYBR Green Supermix (Bio-Rad), 0.25 µL forward primer (100 µM), 0.25 µL reverse primer (100 µM), 8.5 µL dH_2O, and 1.0 µL cDNA template (25 ng/uL). Primer pairs used in PCR reactions include fibronectin (5′- GGTGACACTTATGAGCGCCCTA-3′, 5′-AACATGTAGCCAC CAGTCTCAT-3′), and GAPDH (5′-ACTCCACTCACGG CAAATTC-3′, 5′-TCTCCATGGTGGTGAAGAACA-3′). The PCR program consisted of an initial cycle of 95°C for 60 seconds; 40 cycles of 95°C for 60 seconds, 60°C for 45 seconds, and 72°C for 45 seconds; with a final dissociation curve step. As expected, each primer set generated a single peak dissociation curve. Therefore, real-time PCR cycle threshold (Ct) values were calculated using MxPro ver. 4.0 software (Stratagene, Inc., Santa Clara, CA, USA). To determine expression changes for total FN, Ct values from WT and *Tg-MYOC^{Y437H}* mice were

Investigative Ophthalmology & Visual Science

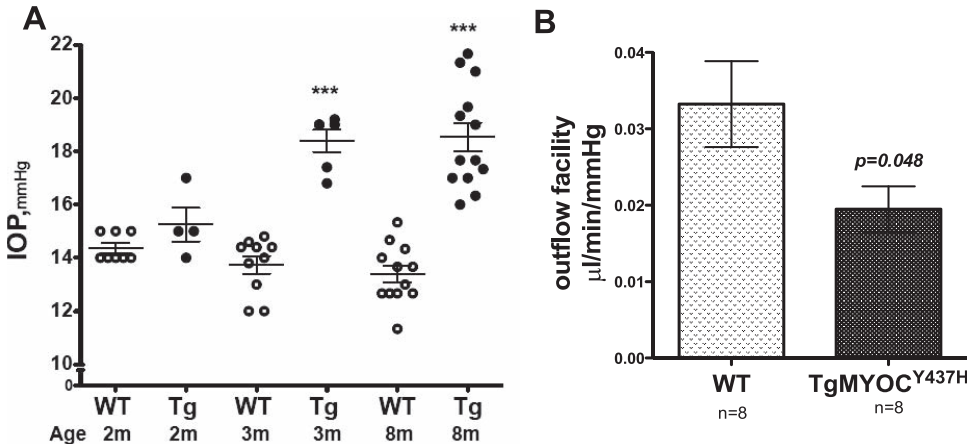

Figure 1. (**A**) Intraocular pressure elevation in 2-, 3-, and 8-month-old WT and *Tg-MYOC*^{Y437H} littermates (two-tailed Student's *t*-test; $^{***}P < 0.0001$; versus WT littermates; $n = 4$–8 eyes at 2 months; $n = 8$–12 eyes for 3 and 8 months). (**B**) Reduced outflow facility in 10-month-old *Tg-MYOC*^{Y437H} mice (two-tailed Student's *t*-test; $P = 0.048$; $n = 8$ eyes).

analyzed using the ΔΔCt method with GAPDH as the normalizing internal control.

Statistical Analysis

All data are represented as mean ± SEM. The data between two groups are analyzed using unpaired two-tailed Student's *t*-test. *P* less than or equal to 0.05 was considered significant. For comparison of ECM proteins between WT and *Tg-MYOC*^{Y437H} mice, 2-way ANOVA was used.

Results

IOP Elevation and Reduced Outflow Facility in Adult *Tg-MYOC*^{Y437H} Mice

Previously, McDowell et al.[41] demonstrated that A/J mice have susceptibility to mutant myocilin induced IOP elevation and optic nerve damage compared with C57BL/6J mice. Therefore, we studied IOP elevation in *Tg-MYOC*^{Y437H} mice on A/J background. Conscious IOP was measured in WT and *Tg-MYOC*^{Y437H} littermates at various ages. Starting from 3 months of age, *Tg-MYOC*^{Y437H} mice showed significant IOP elevation compared with WT littermates. Mean IOP differences between WT and *Tg-MYOC*^{Y437H} littermates were 0.8, 4.6, and 5.1 mm Hg at 2, 3, and 8 months of age, respectively (Fig. 1A).

We next measured outflow facilities in 10-month-old WT and *Tg-MYOC*^{Y437H} littermates (Fig. 1B). Outflow facilities in *Tg-MYOC*^{Y437H} mice were significantly reduced compared with WT littermates (0.019 ± 0.002 vs. 0.033 ± 0.005 µL/min/mm Hg, mean $\Delta = 0.014$ µL/min/mm Hg, $N = 8$ each, $P = 0.048$). Outflow facilities in *Tg-MYOC*^{Y437H} mice were decreased by 42% compared with WT littermates. Conscious IOP measurements in the same mice were increased by approximately 4 mm Hg compared with WT littermates (13.5 mm Hg in WT vs. 17.6 mm Hg in *Tg-MYOC*^{Y437H} littermates, $P < 0.0001$). The reduction in outflow facility correlated well with mean IOP increase assessed by the Goldmann equation considerations.

Increased ECM Protein Levels in the TM of *Tg-MYOC*^{Y437H} Mice

We next explored whether reduced outflow facility in *Tg-MYOC*^{Y437H} mice was associated with increased ECM protein levels in the TM. Western blot and densitometric analysis of anterior segment tissue lysates from above WT and *Tg-MYOC*^{Y437H} littermates demonstrated that fibronectin and collagen IV protein levels were significantly increased in *Tg-MYOC*^{Y437H} mice compared with WT mice (Figs. 2A, 2B). Although elastin and collagen I appear to be increased in the Western blot, this effect was not found significant. Laminin levels were unchanged in *Tg-MYOC*^{Y437H} mice compared with WT littermates. In addition, MMP-2 levels appear to be decreased in *Tg-MYOC*^{Y437H} mice compared with WT mice (although not statistically significant). Immunostaining for collagen I, fibronectin, and collagen type IV was increased in the TM region (shown by arrows) of *Tg-MYOC*^{Y437H} mice compared with WT mice (Fig. 2C). Top panels show bright field images of the same sections indicating TM location (arrows). There was no background staining observed in the TM region of control slides (bottom panel). Quantitative PCR analysis of anterior segment tissues showed no significant change in fibronectin mRNA ($P = 0.098$ two-tailed *t*-test; $n = 5$ each) in *Tg-MYOC*^{Y437H} mice compared with WT littermates (Fig. 2D).

We next sought to examine whether increased ECM protein levels in the TM of *Tg-MYOC*^{Y437H} mice was associated with induction of ER stress and IOP elevation. As shown in Figure 1A, *Tg-MYOC*^{Y437H} mice develop IOP elevation at the age of 3 months. We therefore examined ER stress and fibronectin levels in anterior segment tissues of 2- and 3-month-old WT and *Tg-MYOC*^{Y437H} mice (Figs. 3A, 3B). Western blot analysis demonstrated that expression of mutant myocilin induced ER stress at 2 and 3 months of age as evident from increased Grp78 and CHOP. Fibronectin levels were unchanged at 2 months, but were noticeably increased at 3 months of age. Densitometric analysis (Fig. 3B) demonstrated approximately 1.3-fold increase in Grp78 and CHOP (statistically not significant) but no change in fibronectin levels in 2-month-old *Tg-MYOC*^{Y437H} mice. At 3 months of age, *Tg-MYOC*^{Y437H} mice showed more than 3.5-fold increase in fibronectin ($P < 0.01$) and CHOP ($P < 0.05$) and 2.9-fold increase in Grp78 (statistically not significant) compared with age-matched littermates.

Expression of Mutant Myocilin Leads to Increased Intracellular Accumulation of Selected ECM Proteins in TM-3 Cells

We next examined whether chronic expression of mutant myocilin increases ECM protein levels in cultured TM cells. To study the effects of mutant myocilin in TM cells, we first generated TM-3 cells stably expressing DsRed tagged WT or Y437H mutant myocilin (Fig. 4). Consistent with previous

Investigative Ophthalmology & Visual Science

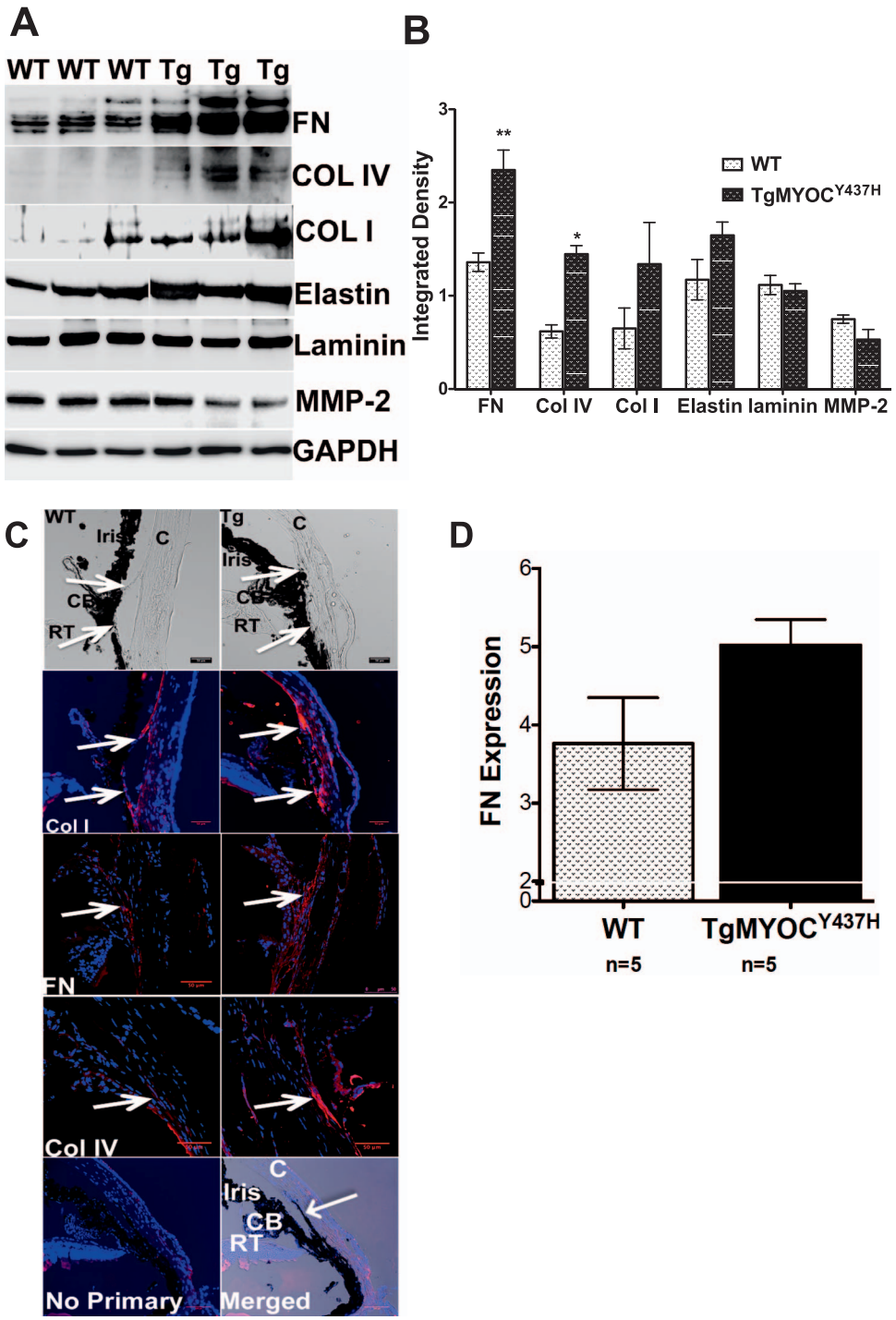

Figure 2. (**A**) Western blot and (**B**) densitometric analysis of fibronectin, elastin, laminin, MMP-2, and collagen types IV and I in anterior segment tissue lysates of 10-month-old WT and *Tg-MYOC*^{Y437H} littermates; $N = 3$ each; $^{*}P < 0.05$, $^{**}P < 0.01$; 2-way ANOVA. (**C**) Immunostaining for collagen I, fibronectin, and collagen IV in the anterior segment of 10-month-old WT and *Tg-MYOC*^{Y437H} littermates ($n = 3$ each); *arrow* shows TM. *Top panel* shows bright field images (with oblique illumination) of anterior segment tissues showing ocular structures. *Arrow* shows TM. *Bottom panel* shows no primary antibody control. (**D**) Quantitative PCR analysis of fibronectin mRNA expression in the anterior segment tissues of 4-month-old WT and *Tg-MYOC*^{Y437H} littermates ($n = 5$ each). Although *Tg-MYOC*^{Y437H} mice show slight increase in fibronectin mRNA expression, this effect was not significant by two-tailed Student's *t*-test. CB, ciliary body; RT, retina; C, cornea.

studies,[26,28,30,42] TM-3 cells stably expressing mutant myocilin show inhibition of myocilin secretion into medium (Fig. 4A) and intracellular accumulation (Fig. 4B) of mutant myocilin. Because serum contains ECM proteins and growth factors, TM cells were cultured with and without serum (0%, 2%, and 10%) to study the effect of mutant myocilin on ER stress and ECM protein levels (Fig. 4C). Western blot analysis of TM cell lysates demonstrated that mutant myocilin induced ER stress as evident from increased GRP78, GRP94, CHOP, and ATF4 levels in both serum and serum-free conditions (Fig. 4C). Increased fibronectin, elastin, and laminin protein levels was also observed in TM-3 cells expressing mutant myocilin in both

Investigative Ophthalmology & Visual Science

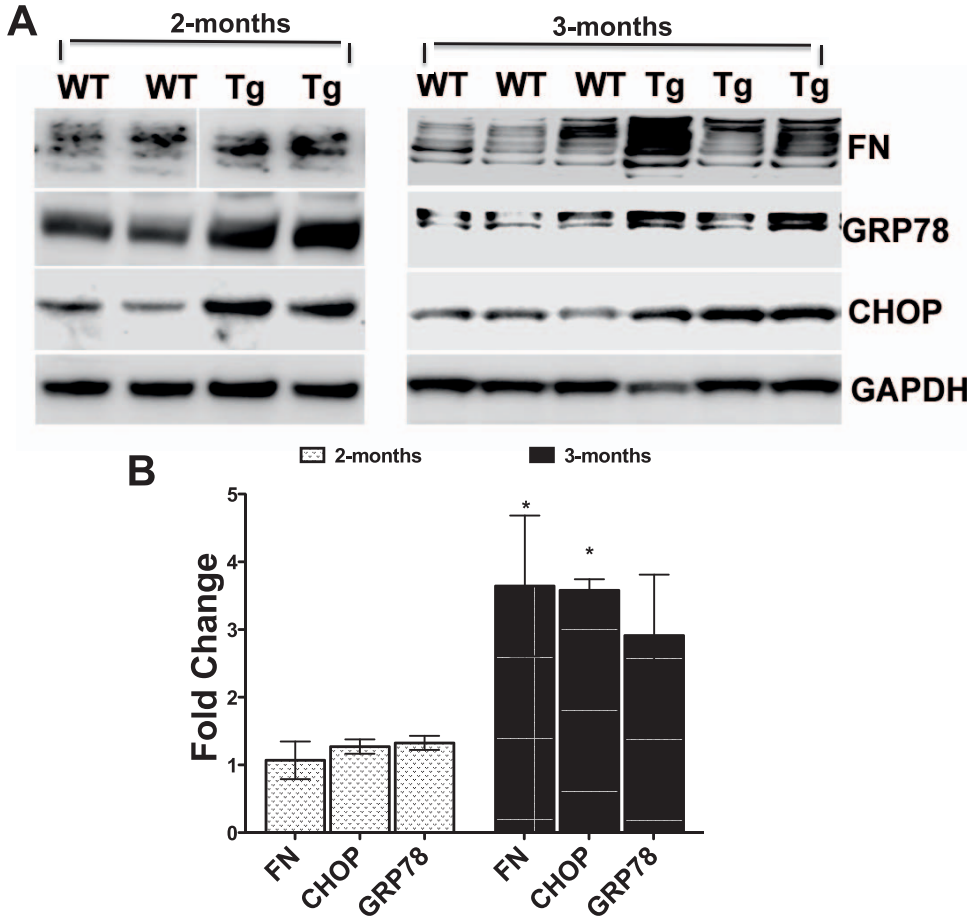

Figure 3. (**A**) Western blot analysis of fibronectin, GRP78, and CHOP in the anterior segment tissue lysates of 2- and 3-month-old WT and *Tg-MYOC*^{Y437H} littermates. Western blot for fibronectin at 2-month time-period are run on the same gel. The lanes were cut and shown in the order presented. (**B**) Densitometric analysis of above proteins in 2- and 3-month-old WT and *Tg-MYOC*^{Y437H} littermates. Expression of each marker was divided by GAPDH (loading control) and fold change in *Tg-MYOC*^{Y437H} mice over WT mice was calculated by dividing values from *Tg-MYOC*^{Y437H} >mice ($n = 4$ at 2 months and $n = 3$ at 3 months) by averaged values from WT mice ($n = 4$ at 2 months and $n = 3$ at 3months). Fibronectin and CHOP were significantly increased in 3-month-old *Tg-MYOC*^{Y437H} mice compared with WT littermates. 2-way ANOVA; $*P < 0.05$; $**P < 0.01$, $n = 3$ each.

serum-free and serum conditions. However, effect of mutant myocilin on ER stress and selected ECM proteins was much pronounced when TM cells were cultured in serum-free medium compared with serum conditions. Interestingly, expression of mutant myocilin reduced both pro and active forms of MMP-2 and slightly increased plasminogen activator inhibitor-1 (PAI-1). This effect was much more pronounced when cells were grown in the absence of serum. However, MMP-9 levels were found unchanged in TM-3 cells expressing mutant myocilin compared with WT myocilin. Western blot analysis of conditioned medium revealed that both pro and active forms of secreted MMP-2 were reduced in TM cells expressing mutant myocilin (Fig. 4D). Interestingly, the active form of MMP-2 was only detected in serum-free conditions. Only the active form of MMP-9 was detected in conditioned medium and was noticeably decreased in TM cells expressing mutant myocilin. In addition, the soluble form of fibronectin was increased in TM-3 cells expressing mutant myocilin grown in serum and serum-free medium. It should be noted that Western blot analysis only detects soluble forms of fibronectin proteins. In addition, TM cells expressing mutant myocilin exhibited inhibition of myocilin secretion while WT myocilin was secreted. These data indicate that expression of mutant myocilin in TM-3 cells induces ER stress, alters secretion, and increases intracellular levels of selected ECM proteins as well as reduces active forms of MMP-2 and –9.

Expression of Mutant Myocilin Increases Intracellular Accumulation of Selected ECM Proteins in Primary Human TM Cells

We next examined whether mutant myocilin expression increases intracellular accumulation of selected ECM proteins in primary TM cells. Primary human TM cells obtained from four different normal donors were transduced with adenoviruses expressing WT MYOC and Y437H mutant MYOC as described previously.[26] Expression of mutant myocilin increased intracellular myocilin accumulation compared with WT myocilin (bottom panel, Fig. 5A). Consistent with transformed TM-3 cells, expression of mutant myocilin also increased intracellular levels of fibronectin, elastin, and collagen type IV compared with WT myocilin in primary TM cells (Fig. 5A). Densitometric analysis of Western blot of selected ECM proteins in conditioned medium revealed more than 3-fold inhibition of mutant myocilin secretion compared with WT myocilin ($P < 0.05$, $n = 4$ each, Fig. 5B). However, fibronectin, collagen type IV, and elastin secretion was not altered in TM cells expressing mutant myocilin compared to TM cells expressing WT myocilin.

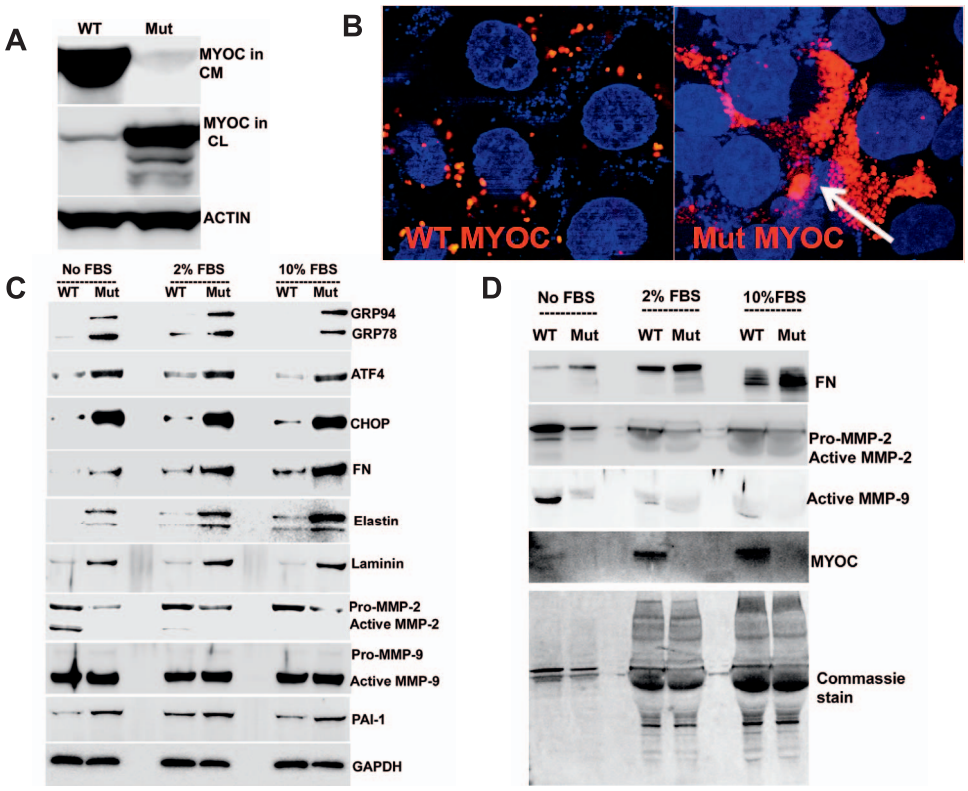

Figure 4. (**A**) Western blot for myocilin in conditioned medium (CM) and cell lysates (CL) of TM cells expressing WT or mutant MYOC. (**B**) Myocilin accumulation and the presence of aggregates (shown by *arrow*) in TM cells stably expressing mutant myocilin. TM-3 cells stably expressing WT or mutant myocilin were grown without serum or with 2% and 10% serum for 48 hours. Total cellular lysates (**C**) or conditioned medium (**D**) was subjected to Western blot analysis of ECM and ER stress proteins. The experiment was repeated twice in TM-3 cells.

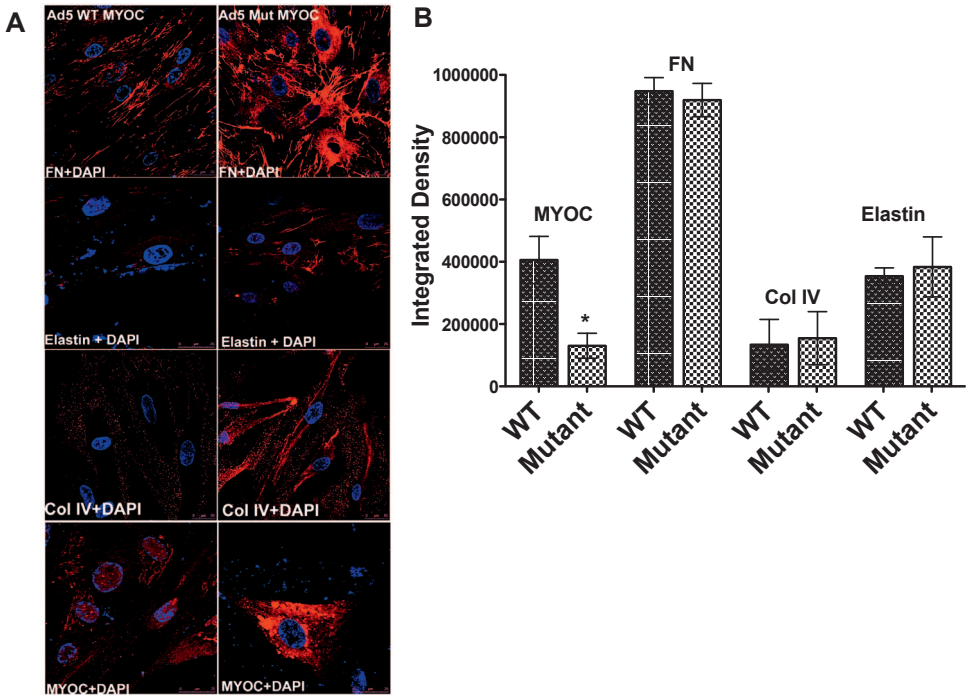

Figure 5. (**A**) Immunostaining for selected ECM proteins in human primary TM cells ($n = 4$ cell strains) transduced with Ad.5 expressing WT or mutant myocilin for 48 hours. Expression of mutant myocilin induced intracellular accumulation of fibronectin, elastin, and collagen IV. (**B**) Densitometric analysis of Western blot of secreted ECM proteins in human primary TM cells. Human primary TM cells ($n = 4$ cell strains) were transfected with plasmid expressing DsRed tagged WT or mutant myocilin using Nucleofector electroporation technology and conditioned medium was subjected to Western blot analysis of selected ECM proteins. Densitometric analysis was performed and integrated density values of each protein are represented graphically. Trabecular meshwork cells expressing mutant myocilin show significant inhibition of myocilin secretion but there was no change in secreted ECM proteins (2-way ANOVA; $^*P < 0.05$; $n = 4$ each).

Investigative Ophthalmology & Visual Science

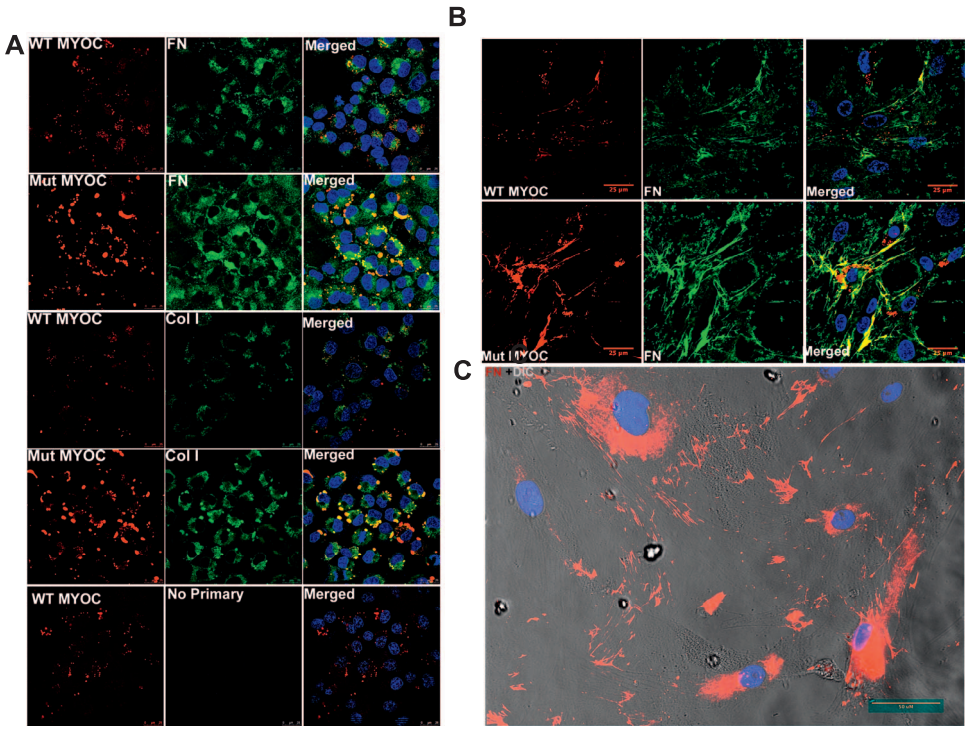

FIGURE 6. **(A)** TM-3 cells stably expressing DsRed tagged WT or mutant myocilin were grown in serum-free medium for 48 hours and stained with FN and Col I antibody. Colocalization of myocilin with fibronectin or collagen I was examined by confocal microscopy. Trabecular meshwork cells incubated without primary antibody shows minimum background staining (*bottom panel*). The experiment was repeated twice in TM-3 cells expressing myocilin. **(B)** Human primary TM cells ($n = 4$ cell strains) were transfected with plasmids expressing DsRed tagged WT or mutant myocilin using nucleofector electroporation technology and cells were cultured for 7 days. Fixed cells were stained with fibronectin and its colocalization was examined by confocal microscopy. **(C)** To determine whether fibronectin staining observed in primary human TM cells ($n = 2$ cell strains) is intracellular or extracellular, human primary TM cells transduced with mutant myocilin was stained with fibronectin and merged with bright-field image. Merged images show that almost the entire fibronectin staining was intracellular.

Mutant Myocilin-Induced ECM Proteins Colocalize With Mutant Myocilin and Accumulate Intracellularly in the ER of TM Cells

A previous study by Filla et al.[23] demonstrated that myocilin colocalizes with fibronectin, laminin, and collagen type IV in Dex-treated TM cells. We therefore examined whether mutant myocilin colocalizes with selected ECM proteins in TM cells. We first examined colocalization of myocilin with fibronectin and collagen I in TM-3 cells stably expressing WT or mutant myocilin (Fig. 6A). A small amount of colocalization of WT myocilin with fibronectin or collagen I was observed in TM cells expressing WT myocilin. However, there was increased colocalization of mutant myocilin with fibronectin and collagen I in TM cells expressing mutant myocilin. In addition, a similar pattern of colocalization of fibronectin with mutant myocilin was observed in primary human TM cells transfected with DsRed-tagged mutant myocilin (Fig. 6B). Although some of the fibronectin staining appeared to be extracellular, colocalization with bright field images revealed that most of fibronectin staining was intracellular (Fig. 6C).

Because mutant myocilin accumulates intracellularly in the ER, we next examined whether fibronectin and collagen type I also accumulate in the ER (Fig. 7). Human primary TM cells transduced with Ad.5 expressing WT or mutant myocilin were stained with FN or collagen type I (green) along with ER marker KDEL (red). Little or no colocalization of fibronectin or collagen type I with KDEL was observed in TM cells expressing WT myocilin. However, a strong colocalization of fibronectin and collagen type I staining was observed with KDEL in TM cells expressing mutant myocilin indicating accumulation of these selected ECM proteins in the ER of primary TM cells (Fig. 7A).

We next examined whether expression of mutant myocilin in *Tg-MYOC^{Y437H}* mice induces intracellular accumulation of fibronectin in TM tissues. Using ×63-lens objective of confocal microscope, we examined fibronectin immunostaining in WT and *Tg-MYOC^{Y437H}* mice. As shown in the top panel (Fig. 7B), some of fibronectin immunostaining appears to be perinuclear and there was increased fibronectin perinuclear staining in *Tg-MYOC^{Y437H}* mice ($n = 4$ each). To further examine whether there is increased intracellular accumulation of fibronectin in the ER of TM cells, we examined colocalization of fibronectin with KDEL (ER marker). As shown in the bottom panel, there was increased colocalization of fibronectin with KDEL in *Tg-MYOC^{Y437H}* mice indicating intracellular accumulation of fibronectin in the ER of TM in *Tg-MYOC^{Y437H}* mice.

Inhibiting ER Stress Via Sodium 4-phenylbutyrate (PBA) Reduced Mutant Myocilin-Induced Intracellular Accumulation of ECM Proteins in TM Cells

We next examined whether reducing ER stress associated with mutant myocilin rescues increased intracellular ECM accumulation in TM cells. TM-3 cells stably expressing mutant myocilin were treated with 5 mM PBA for 48 hours, and cell lysates were subjected to Western blot analysis of ER stress markers and selected ECM proteins. Treatment with PBA reduced mutant myocilin intracellular accumulation, decreased ER stress markers, and reduced ECM proteins (Fig. 8A). Sodium 4-phenylbutyrate treatment did not alter fibronectin staining in

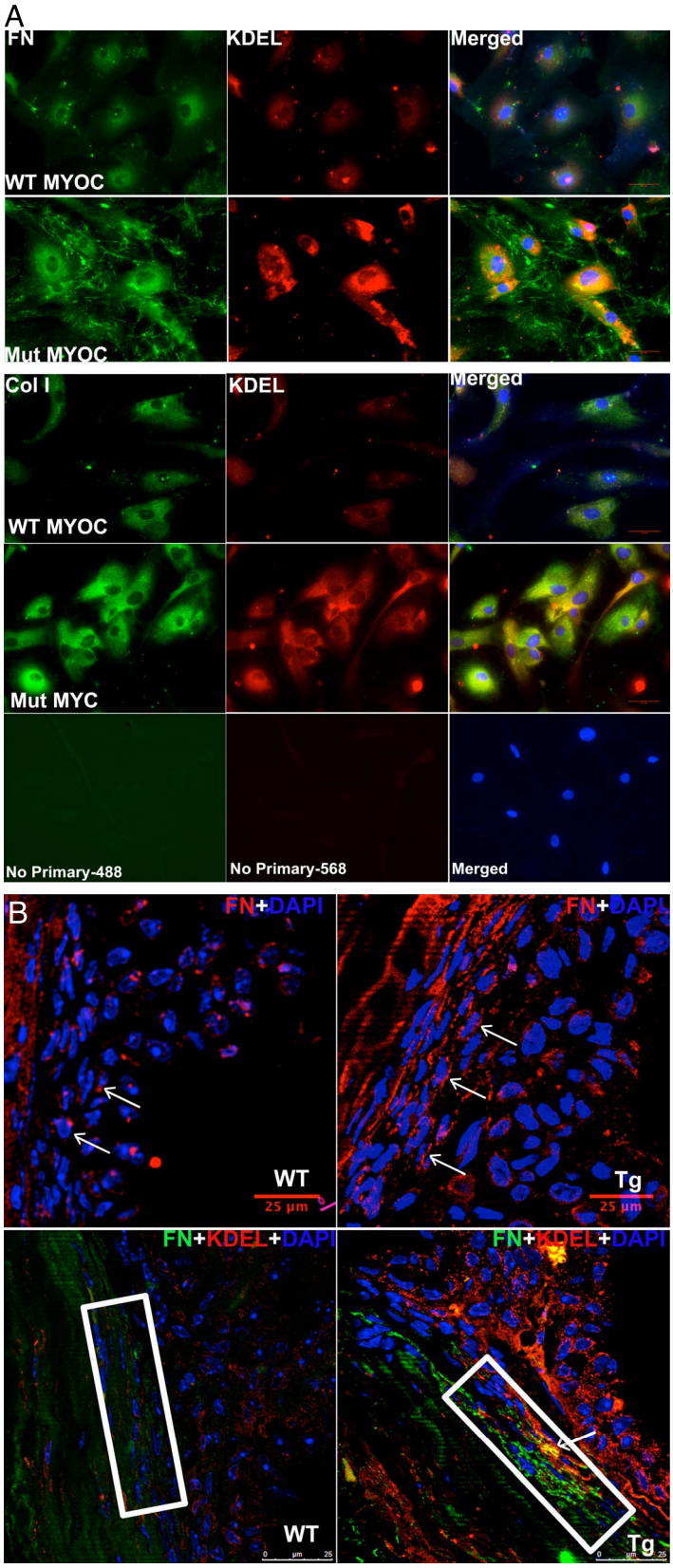

Figure 7. (**A**) Human primary TM cells ($n = 3$ cell strains) transduced with Ad.5 expressing WT or mutant myocilin were costained with fibronectin (FN) or collagen I (Col I) along with ER marker KDEL. Colocalization of fibronectin or collagen I with KDEL was examined by confocal microscopy. Trabecular meshwork cells incubated without primary antibody (*bottom panel*) showed minimum background staining for above antibodies. Increased accumulation of fibronectin and collagen I in the ER was observed in TM cells expressing mutant myocilin. (**B**) Higher magnification images of fibronectin immunostaining in the anterior segment of 3-month-old WT and *Tg-MYOC*^{Y437H} littermates ($n = 4$ each) is shown in the *top panel*. *Arrows* show perinuclear-staining pattern of fibronectin in both WT and *Tg-MYOC*^{Y437H} mice. *Bottom panel* shows double immunostaining of anterior segment with fibronectin (*green*) and KDEL (*red*) in 3-month-old WT and *Tg-MYOC*^{Y437H} littermates. *Rectangular box* shows TM region and *arrows* show colocalization of fibronectin with ER marker KDEL in the TM cells of *Tg-MYOC*^{Y437H} mice.

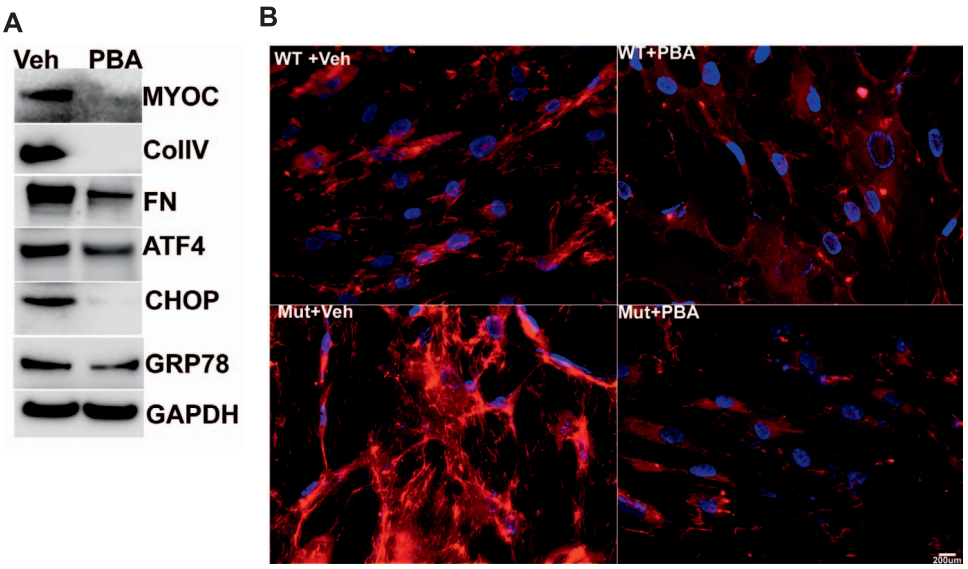

Figure 8. (**A**) TM-3 cells stably expressing mutant myocilin were treated with or without PBA (5 mM) and cell lysates were subjected to Western blot analysis of ECM and ER stress proteins. Western blot was repeated twice in TM-3 cells expressing mutant myocilin. (**B**) Immunostaining for fibronectin in primary human TM cells transduced with Ad5 expressing WT or mutant myocilin and treated with or without PBA for 48 hours ($n = 4$ cell strains). Sodium 4-phenylbutyrate treatment reduced ER stress and also decreased selected ECM proteins in TM cells.

primary TM cells transduced with WT myocilin. However, PBA reduced intracellular fibronectin levels induced by mutant myocilin in primary TM cells (Fig. 8B).

Discussion

Abnormal accumulation of ECM proteins in the TM is associated with reduced aqueous humor outflow facility (or increased outflow resistance) and IOP elevation in glaucoma. It is not understood whether mutant myocilin, a known cause of POAG, alters ECM in the TM and reduces outflow facility. In the present study, we show that the expression of mutant myocilin in the TM of *Tg-MYOC*^{Y437H} mice leads to reduced outflow facility and IOP elevation. Reduced outflow facility is associated with increased ECM protein levels in the TM of *Tg-MYOC*^{Y437H} mice. Also, increased fibronectin in the TM is associated with chronic ER stress. Using human TM-3 cells stably expressing mutant myocilin and primary TM cells transduced with Ad5 expressing mutant myocilin, we show that expression of mutant myocilin induces ER stress, alters secretion and increases intracellular retention of selected ECM proteins as well as reduces active forms of MMP-2 and –9. Interestingly, mutant myocilin induced ECM proteins colocalize with mutant myocilin and an ER marker, indicating intracellular accumulation of these proteins in the ER of TM cells. Reduction of ER stress prevents mutant myocilin-induced ECM accumulation in TM cells.

It is well accepted that reduced aqueous humor outflow facility leads to IOP elevation in POAG patients. Wilkinson et al.[43] demonstrated a reduction in outflow facility in carriers of myocilin mutations even prior to developing glaucoma. In our study, we show that mutant myocilin reduces outflow facility in *Tg-MYOC*^{Y437H} mice. The measured mean IOP increase of approximately 4 mm Hg in *Tg-MYOC*^{Y437H} mice compared to WT mice corresponded very closely with the mean reduction in outflow facility of approximately 42%, according to the Goldmann equation. Together, our studies suggest that reduced outflow facility in *Tg-MYOC*^{Y437H} mice may be responsible for IOP elevation and development of POAG.

It is thought that abnormal ECM accumulation in the TM impairs outflow facility, thus elevating IOP. Consistent with this, we observed significantly increased intracellular accumulation of selected ECM proteins including fibronectin and collagen IV and I in the TM of *Tg-MYOC*^{Y437H} mice. Although fibronectin mRNA expression appears to be increased slightly in *Tg-MYOC*^{Y437H} mice, this effect was not statically significant. In addition, we observed increased intracellular retention of fibronectin, collagen IV, and elastin in the ER of TM cells. Together, these findings suggest that mutant myocilin induced increase in ECM may be a post translational effect.

Mechanical stress induced by IOP elevation has been shown to stimulate ECM deposition in the TM.[44] Therefore, chronic IOP elevation in *Tg-MYOC*^{Y437H} mice could also alter ECM composition in the TM. Because fibronectin levels were increased only in ocular hypertensive *Tg-MYOC*^{Y437H} mice, it is possible that elevated IOP can increase ECM accumulation in TM. However, expression of mutant myocilin also increased abnormal ECM accumulation in human primary TM cells indicating that expression of mutant myocilin alone is sufficient to induce abnormal ECM accumulation.

In this study, we also generated TM cells stably expressing DsRed-tagged WT or mutant myocilin. Similar to our previous studies, mutant myocilin inhibits its secretion and accumulates intracellularly, inducing ER stress. Thus, these cells precisely recapitulate mutant myocilin gain-of-function phenotype. Generation of these TM cells provides a valuable tool to further investigate how protein misfolding and ER stress induced by mutant myocilin modulates ECM proteins and leads to TM dysfunction. Interestingly, TM-3 stable cells expressing mutant myocilin also demonstrated increased abnormal accumulation of ECM proteins similar to *Tg-MYOC*^{Y437H} mice. Specifically, expression of mutant myocilin increased intracellular levels of fibronectin, collagens, and elastin. Although no change in laminin and the effect on elastin was moderate in *Tg-MYOC*^{Y437H} mice, we observed a considerable increase in intracellular laminin and elastin protein levels in TM-3 cells expressing mutant myocilin. Because Western blot analysis of these proteins in *Tg-MYOC*^{Y437H} mice was performed using anterior segment tissues, which also includes other ocular tissues, this effect may be diluted in Western blot analysis in mouse tissues compared with the TM-3 cell line. In addition, a similar pattern

Investigative Ophthalmology & Visual Science

of increased intracellular ECM accumulation was observed in primary human TM cells expressing mutant myocilin. In contrast to TM-3 cells stably expressing mutant myocilin, expression of mutant myocilin did not increase secretion of soluble ECM proteins into the conditioned medium. It is possible that stable and chronic expression of mutant myocilin in TM-3 cells activates certain pathways over time, leading to increased secretion of ECM compared with transient expression of mutant myocilin in human primary TM cells.

Matrix metalloproteinases regulate the turnover of ECM proteins in TM cells. Tissue inhibitors of metalloproteinases (TIMP) and PAI-1 also regulate ECM deposition by regulating MMP activity.[45] Treatment of TM cells with TGF-β2 has been shown to increase MMP-2 and PAI-1.[16] Some studies have suggested that reduced MMP activity is involved in increased ECM deposition observed in glaucomatous TM tissues.[46–48] In the human ex vivo anterior segment perfusion system, MMPs increased outflow facility.[48] It is interesting to note that mutant myocilin reduced the active forms of MMP-2 and –9. Because MMPs can degrade ECM proteins, reduced MMP activity can result in altered deposition of ECM in TM cells expressing mutant myocilin. In addition, we observed that expression of mutant myocilin increased PAI-1, which may be responsible for decreased MMP-2 and –9. Together, these data suggest that expression of mutant myocilin may alter the ECM composition in the TM cells.

Consistent with our hypothesis, several findings from our current study suggest that mutant myocilin causes intracellular retention of selected ECM proteins in the ER of TM cells. Western blot (Fig. 4A) and immunostaining (Figs. 5A, 6A–C, and 7) show that expression of mutant myocilin increases intracellular ECM proteins in TM-3 cells lysates and primary TM cells. A considerable colocalization of fibronectin or collagen I with mutant myocilin is observed in TM cells expressing mutant myocilin and most of this colocalization is found in myocilin aggregates (Figs. 6A, 6B). Also, most of fibronectin immunostaining observed in primary TM cells expressing mutant myocilin appears to be intracellular (Fig. 6C). Both fibronectin and collagen I colocalized strongly with ER marker KDEL (Fig. 7), suggesting intracellular accumulation of these ECM proteins in the ER of TM cells. In addition, immunostaining of anterior segment tissues of *Tg-MYOC^{Y437H}* mice demonstrates an intracellular accumulation of ECM proteins in the TM. Although it is not clear how mutant myocilin causes intracellular retention of these ECM proteins, it is possible that mutant myocilin may bind nonspecifically to these selected ECM proteins in the aggregates, causing additional ER stress to TM cells. Also, chronic ER stress induced by mutant myocilin may overwhelm normal folding and quality control machinery in the ER, thus not allowing proper folding of these ECM proteins. In addition, accumulation of these selected ECM proteins may further worsen ongoing ER stress due to mutant myocilin. These events may lead to TM dysfunction and cell loss over time causing reduced outflow facility and IOP elevation. Considering the role of WT myocilin in cell–matrix interactions, it is possible that inhibition of myocilin secretion activates a compensatory feedback mechanism to enhance ECM synthesis and secretion. A previous study suggested role of myocilin as a molecular chaperone[49] and lack of chaperone activity in the case of mutant myocilin may also cause intracellular retention of selected ECM proteins.

Previously, we have shown that protein misfolding induced by mutant myocilin induces ER stress in the TM, which is associated with IOP elevation.[26] Consistent with our previous studies, we observed increased ER stress markers in the anterior segment of *Tg-MYOC^{Y437H}* mice and TM cells expressing mutant myocilin. Interestingly, increased ECM proteins were also associated with these ER stress markers. Moreover, reduction in ER stress via PBA dramatically reduced ECM accumulation induced by mutant myocilin in primary human TM cells. It is thus possible that ER stress induced by mutant myocilin is responsible for increased ECM. Extracellular matrix proteins are processed in the ER for secretion. A change in ER homeostasis due to misfolded protein may alter secretion and deposition in of these ECM proteins. Consistent with this hypothesis, we have previously shown that reduction of ER stress via PBA reduced Dex-induced IOP elevation and also significantly decreased Dex-induced fibronectin accumulation in the TM.[33] Recently, we have shown that ER stress prodeath markers ATF4 and CHOP are significantly increased in the human glaucomatous TM tissues and cells.[50] It is plausible that induction of ATF4 and CHOP may play a critical role in ECM remodeling in human glaucomatous TM tissues. Our future studies will be aimed at understanding whether ER stress can modify ECM deposition in the TM.

Overall, our studies clearly demonstrate the role of mutant myocilin in increased intracellular abnormal ECM accumulation in the TM and altered secretion, which may result in TM dysfunction, reduced outflow facility, and IOP elevation. Our study further suggests the role of protein misfolding and ER stress in regulation of ECM.

Acknowledgments

The authors would like to thank Abbot Clark, PhD, for donating primary TM cells and sharing reagents.

Supported by grants from the National Eye Institute (Bethesda, MD, USA), EY022077 (R00; GSZ) and EY026177 (R01; GSZ) and funding from the North Texas Eye Research Institute (Fort Worth, TX, USA).

Disclosure: **R.B. Kasetti**, None; **T.N. Phan**, None; **J.C. Millar**, None; **G.S. Zode**, None

References

1. Quigley HA, Broman AT. The number of people with glaucoma worldwide in 2010 and 2020. *Br J Ophthalmol*. 2006;90:262–267.
2. Quigley HA. Neuronal death in glaucoma. *Prog Retin Eye Res*. 1999;18:39–57.
3. Rosenthal J, Leske MC. Open-angle glaucoma risk factors applied to clinical area. *J Am Optom Assoc*. 1980;51:1017–1024.
4. Kwon YH, Fingert JH, Kuehn MH, Alward WL. Primary open-angle glaucoma. *N Engl J Med*. 2009;360:1113–1124.
5. Rohen JW. Why is intraocular pressure elevated in chronic simple glaucoma? Anatomical considerations. *Ophthalmology*. 1983;90:758–765.
6. Rohen JW, Lutjen-Drecoll E, Flugel C, Meyer M, Grierson I. Ultrastructure of the trabecular meshwork in untreated cases of primary open-angle glaucoma (POAG). *Exp Eye Res*. 1993;56:683–692.
7. Lutjen-Drecoll E, Rittig M, Rauterberg J, Jander R, Mollenhauer J. Immunomicroscopical study of type VI collagen in the trabecular meshwork of normal and glaucomatous eyes. *Exp Eye Res*. 1989;48:139–147.
8. Medina-Ortiz WE, Belmares R, Neubauer S, Wordinger RJ, Clark AF. Cellular fibronectin expression in human trabecular meshwork and induction by transforming growth factor-beta2. *Invest Ophthalmol Vis Sci*. 2013;54:6779–6788.
9. Alvarado J, Murphy C, Juster R. Trabecular meshwork cellularity in primary open-angle glaucoma and nonglaucomatous normals. *Ophthalmology*. 1984;91:564–579.
10. Gong HY, Trinkaus-Randall V, Freddo TF. Ultrastructural immunocytochemical localization of elastin in normal human trabecular meshwork. *Curr Eye Res*. 1989;8:1071–1082.
11. Vranka JA, Kelley MJ, Acott TS, Keller KE. Extracellular matrix in the trabecular meshwork: intraocular pressure regulation and dysregulation in glaucoma. *Exp Eye Res*. 2015;133:112–125.

12. Guo MS, Wu YY, Liang ZB. Hyaluronic acid increases MMP-2 and MMP-9 expressions in cultured trabecular meshwork cells from patients with primary open-angle glaucoma. *Mol Vis*. 2012;18:1175–1181.
13. De Groef L, Van Hove I, Dekeyster E, Stalmans I, Moons L. MMPs in the trabecular meshwork: promising targets for future glaucoma therapies? *Invest Ophthalmol Vis Sci*. 2013; 54:7756–7763.
14. Acott TS, Kelley MJ. Extracellular matrix in the trabecular meshwork. *Exp Eye Res*. 2008;86:543–561.
15. Pang IH, Hellberg PE, Fleenor DL, Jacobson N, Clark AF. Expression of matrix metalloproteinases and their inhibitors in human trabecular meshwork cells. *Invest Ophthalmol Vis Sci*. 2003;44:3485–3493.
16. Fuchshofer R, Welge-Lussen U, Lutjen-Drecoll E. The effect of TGF-beta2 on human trabecular meshwork extracellular proteolytic system. *Exp Eye Res*. 2003;77:757–765.
17. Clark AF, Miggans ST, Wilson K, Browder S, McCartney MD. Cytoskeletal changes in cultured human glaucoma trabecular meshwork cells. *J Glaucoma*. 1995;4:183–188.
18. Hoare MJ, Grierson I, Brotchie D, Pollock N, Cracknell K, Clark AF. Cross-linked actin networks (CLANs) in the trabecular meshwork of the normal and glaucomatous human eye in situ. *Invest Ophthalmol Vis Sci*. 2009;50:1255–1263.
19. Stone EM, Fingert JH, Alward WL, et al. Identification of a gene that causes primary open angle glaucoma. *Science*. 1997;275: 668–670.
20. Aroca-Aguilar JD, Sanchez-Sanchez F, Ghosh S, Fernandez-Navarro A, Coca-Prados M, Escribano J. Interaction of recombinant myocilin with the matricellular protein SPARC: functional implications. *Invest Ophthalmol Vis Sci*. 2011;52: 179–189.
21. Hardy KM, Hoffman EA, Gonzalez P, McKay BS, Stamer WD. Extracellular trafficking of myocilin in human trabecular meshwork cells. *J Biol Chem*. 2005;280:28917–28926.
22. Clark AF, Steely HT, Dickerson JE Jr, et al. Glucocorticoid induction of the glaucoma gene MYOC in human and monkey trabecular meshwork cells and tissues. *Invest Ophthalmol Vis Sci*. 2001;42:1769–1780.
23. Filla MS, Liu X, Nguyen TD, et al. In vitro localization of TIGR/MYOC in trabecular meshwork extracellular matrix and binding to fibronectin. *Invest Ophthalmol Vis Sci*. 2002;43: 151–161.
24. Sohn S, Joe MK, Kim TE, et al. Dual localization of wild-type myocilin in the endoplasmic reticulum and extracellular compartment likely occurs due to its incomplete secretion. *Mol Vis*. 2009;15:545–556.
25. Tamm ER. Myocilin and glaucoma: facts and ideas. *Prog Retin Eye Res*. 2002;21:395–428.
26. Zode GS, Kuehn MH, Nishimura DY, et al. Reduction of ER stress via a chemical chaperone prevents disease phenotypes in a mouse model of primary open angle glaucoma. *J Clin Invest*. 2011;121:3542–3553.
27. Liu Y, Vollrath D. Reversal of mutant myocilin non-secretion and cell killing: implications for glaucoma. *Hum Mol Genet*. 2004;13:1193–1204.
28. Jacobson N, Andrews M, Shepard AR, et al. Non-secretion of mutant proteins of the glaucoma gene myocilin in cultured trabecular meshwork cells and in aqueous humor. *Hum Mol Genet*. 2001;10:117–125.
29. Gobeil S, Rodrigue MA, Moisan S, et al. Intracellular sequestration of hetero-oligomers formed by wild-type and glaucoma-causing myocilin mutants. *Invest Ophthalmol Vis Sci*. 2004;45:3560–3567.
30. Joe MK, Sohn S, Hur W, Moon Y, Choi YR, Kee C. Accumulation of mutant myocilins in ER leads to ER stress and potential cytotoxicity in human trabecular meshwork cells. *Biochem Biophys Res Commun*. 2003;312:592–600.
31. Anholt RR, Carbone MA. A molecular mechanism for glaucoma: endoplasmic reticulum stress and the unfolded protein response. *Trends Mol Med*. 2013;19:586–593.
32. Yam GH, Gaplovska-Kysela K, Zuber C, Roth J. Aggregated myocilin induces russell bodies and causes apoptosis: implications for the pathogenesis of myocilin-caused primary open-angle glaucoma. *AM J Pathol*. 2007;170:100–109.
33. Zode GS, Sharma AB, Lin X, et al. Ocular-specific ER stress reduction rescues glaucoma in murine glucocorticoid-induced glaucoma. *J Clin Invest*. 2014;124:1956–1965.
34. Wang WH, Millar JC, Pang IH, Wax MB, Clark AF. Noninvasive measurement of rodent intraocular pressure with a rebound tonometer. *Invest Ophthalmol Vis Sci*. 2005;46:4617–4621.
35. Millar JC, Clark AF, Pang IH. Assessment of aqueous humor dynamics in the mouse by a novel method of constant-flow infusion. *Invest Ophthalmol Vis Sci*. 2011;52:685–694.
36. Millar JC, Phan TN, Pang IH, Clark AF. Strain and age effects on aqueous humor dynamics in the mouse. *Invest Ophthalmol Vis Sci*. 2015;56:5764–5776.
37. Wordinger RJ, Fleenor DL, Hellberg PE, et al. Effects of TGF-beta2, BMP-4 and gremlin in the trabecular meshwork: implications for glaucoma. *Invest Ophthalmol Vis Sci*. 2007; 48:1191–1200.
38. Elmore JM, Coaker G. Biochemical purification of native immune protein complexes. *Methods Mol Biol*. 2011;712:31–44.
39. Zode GS, Clark AF, Wordinger RJ. Activation of the BMP canonical signaling pathway in human optic nerve head tissue and isolated optic nerve head astrocytes and lamina cribrosa cells. *Invest Ophthalmol Vis Sci*. 2007;48:5058–5067.
40. Xue W, Comes N, Borras T. Presence of an established calcification marker in trabecular meshwork tissue of glaucoma donors. *Invest Ophthalmol Vis Sci*. 2007;48:3184–3194.
41. McDowell CM, Luan T, Zhang Z, et al. Mutant human myocilin induces strain specific differences in ocular hypertension and optic nerve damage in mice. *Exp Eye Res*. 2012; 100:65–72.
42. Gould DB, Reedy M, Wilson LA, Smith RS, Johnson RL, John SW. Mutant myocilin nonsecretion in vivo is not sufficient to cause glaucoma. *Mol Cell Biol*. 2006;26:8427–8436.
43. Wilkinson CH, van der Straaten D, Craig JE, et al. Tonography demonstrates reduced facility of outflow of aqueous humor in myocilin mutation carriers. *J Glaucoma*. 2003;12:237–242.
44. Liton PB, Liu X, Challa P, Epstein DL, Gonzalez P. Induction of TGF-beta1 in the trabecular meshwork under cyclic mechanical stress. *J Cell Physiol*. 2005;205:364–371.
45. Nagase H. Activation mechanisms of matrix metalloproteinases. *Biol Chem*. 1997;378:151–160.
46. Samples JR, Alexander JP, Acott TS. Regulation of the levels of human trabecular matrix metalloproteinases and inhibitor by interleukin-1 and dexamethasone. *Invest Ophthalmol Vis Sci*. 1993;34:3386–3395.
47. Alexander JP, Samples JR, Van Buskirk EM, Acott TS. Expression of matrix metalloproteinases and inhibitor by human trabecular meshwork. *Invest Ophthalmol Vis Sci*. 1991;32:172–180.
48. Bradley JM, Vranka J, Colvis CM, et al. Effect of matrix metalloproteinases activity on outflow in perfused human organ culture. *Invest Ophthalmol Vis Sci*. 1998;39:2649–2658.
49. Anderssohn AM, Cox K, O'Malley K, et al. Molecular chaperone function for myocilin. *Invest Ophthalmol Vis Sci*. 2011;52:7548–7555.
50. Peters JC, Bhattacharya S, Clark AF, Zode GS. Increased endoplasmic reticulum stress in human glaucomatous trabecular meshwork cells and tissues. *Invest Ophthalmol Vis Sci*. 2015;56:3860–3868.

Investigative Ophthalmology & Visual Science